

Title: X10 Expansion Microscopy Enables 25 nm Resolution on Conventional Microscopes

Authors: Sven Truckenbrodt^{1,2,*}, Manuel Maidorn^{1,2}, Dagmar Crzan¹, Hanna Wildhagen¹, Selda Kabatas¹, Silvio O. Rizzoli^{1,*}

Affiliations:

¹Institute for Neuro- and Sensory Physiology, Center for Biostructural Imaging of Neurodegeneration, University Medical Center Göttingen, Cluster of Excellence Nanoscale Microscopy and Molecular Physiology of the Brain, Göttingen, Germany

²International Max Planck Research School for Molecular Biology, Göttingen, Germany

*correspondence to: Sven Truckenbrodt (strucke@gwdg.de), Silvio O. Rizzoli (srizzol@gwdg.de)

This submission includes:

- Main Text
- 3 Main Figures
- Main Figure Legends
- Supplementary Materials: 9 Supplementary Figures, Supplementary Figure Legends, and Materials & Methods

Main Text:

We present here an improved protocol for expansion microscopy, which increases the expansion factor of the gel from $\sim 4\times$ to $\sim 10\times$. This protocol, which we termed X10 microscopy, achieves a resolution of 25-30 nm, and offers multi-colour imaging, using off-the-shelf reagents and conventional epifluorescence microscopes. This enables a level of imaging detail approaching that of much more challenging methods, such as STED, STORM and iExM, in both cell cultures and tissues.

Expansion microscopy (ExM) is a recently introduced imaging technique that achieves super-resolution through physically expanding the specimen by $\sim 4\times$, after embedding into a swellable gel¹⁻⁴. The resolution attained is, correspondingly, approximately 4-fold better than what the diffraction limit imposes on non-expanded samples, or ~ 70 nm when using conventional epifluorescence microscopes. This is a major improvement over conventional microscopy, but still lags behind modern STED or STORM setups, whose resolution can reach 20-30 nm. We addressed this issue here by introducing an improved gel recipe that enables an expansion factor of 10x, or more, in each dimension, which corresponds to an expansion of the sample volume by more than 1000-fold. This technique, which we termed X10 (incorporating the increased expansion factor in the acronym), thus achieves a resolution of up to ~ 25 nm on conventional epifluorescence microscopes.

We adapted a superabsorbent hydrogel designed for excellent mechanical sturdiness⁵ for the expansion of biological samples. This gel uses *N,N*-dimethyl-acrylamide (DMAA) for generating polymer chains, which are crosslinked with sodium acrylate (SA) to produce a swellable gel matrix (Fig. 1a). The gelation reaction is catalysed by potassium persulfate (KPS) and tetramethyl-ethylene-diamine (TEMED; Supplementary Fig. 1), and produces a gel that can expand $>10\times$ in each dimension when placed in distilled water. The expansion factor is scalable, and depends on the ratio of DMAA to SA⁵. The maximum expansion factor we achieved was 11.5x (Fig. 1b,e; Online Methods), which results in images with an apparent lateral resolution of ~ 25 -30 nm (Fig. 1c,d,h; resolution predicted from Abbe's resolution limit), in which substantially more details are revealed (Fig. 1f).

The resulting technique is fully compatible with the use of common affinity probes, such as antibodies (Fig. 1b,c), since X10, similar to the latest updates on "classical" 4x ExM^{2,6}, requires no specially designed labelling tools. The distortions of the sample introduced by the gel during swelling are minimal (Fig. 1d,g), comparable to those previously described in 4x ExM^{1,2,6}. We would like to point out, however, that the use of the established 4x protocols with the X10 gel recipe may result in significant damage to the sample, through incomplete

polymerization or insufficient digestion. The precise implementation of the protocol we have optimized should avoid these artefacts (Supplementary Fig. 2; Online Methods). We would like to note that X10 once more highlights the need for new probes for super-resolution imaging, as conventional off-the-shelf antibodies usually do not result in a continuous staining of microtubules, but a pearls-on-a-string pattern (Fig. 1c,d). This artefact, which is due to incomplete epitope coverage through conventional antibodies^{7,8}, is not specific to expansion microscopy, as it can be observed also in other super-resolution techniques, such as STED^{7,9-12} and STORM^{13-16,11} (Supplementary Fig. 3).

To verify the resolution of X10 experimentally, we relied on investigating peroxisomes, which are spherical organelles of relatively constant size (~100-200 nm in neurons). We immunostained Pmp70, a protein of the peroxisomes membrane (Fig. 2), and we compared pre-expansion images with post-expansion images as well as with STED and STORM images (Fig. 2a; see Supplementary Fig. 4 for a more detailed comparison). To obtain the nominal resolution of X10, we drew line scans through the membranes of the post-expansion peroxisomes, fitted them to Gaussian curves, and determined their full width at half maximum values (FWHM; Fig. 2b). The resolution we experimentally determined in this fashion fits the theoretical prediction from Abbe's resolution limit that we have stated above, being centred at 25.2 ± 0.2 nm (Fig. 2c). We also simulated peroxisomes stained for Pmp70, taking into account the size and random orientation of the primary/secondary antibody complexes (Supplementary Fig. 5; see Online Methods for details), and found that the measured resolution value fits closely to the one predicted by the simulations (23.8 nm, on 10,000 simulated peroxisomes). This level of resolution is usually only achieved in highly specialized applications of STED and STORM microscopy^{17,18}, and is bettered substantially only by a recently developed tool, MINFLUX microscopy¹⁹. In state-of-the-art commercial STED and STORM setups, the resolution achieved is, at best, comparable to that of X10 (Fig. 2a; Supplementary Fig. 4).

We used this model to determine if we could, theoretically, resolve the lumen of microtubules, but found that this is beyond the limits of X10 at the moment (Supplementary Fig. 5a). Simulations indicated that this is due to problems in the placement of antibodies across the expanded microtubule. Their large size effectively limits resolution, and prevents the measurement of a clear lumen. To observe this lumen, one would require an expansion factor of 15x or more, as recently achieved with iterative ExM (iExM)²⁰, which we will further discuss below. At the same time, this implies that the ~25 nm resolution is possibly the maximum useful resolution that can be achieved in expansion microscopy when using conventional primary/secondary antibody complexes – the probe size and fluorophore/target

distance become the limiting factor, rather than the expansion factor^{20,21} (also see Supplementary Fig. 5). This problem has been noted for super-resolution imaging in the past⁸, but must receive additional attention in view of the ease with which expansion microscopy reaches this limit.

The X10 procedure can be used to achieve multi-colour super-resolution imaging. We could easily resolve, for example, synaptic vesicles in cultured hippocampal neurons, along with the presynaptic active zones and the postsynaptic densities (Fig. 3a,b). These structures were detected by conventional primary antibodies, which were revealed by secondary antibodies conjugated to three different fluorophores. This enabled us to measure the distance between the presynaptic active zone, identified by Bassoon, and the postsynaptic density, identified by Homer 1 (Fig. 3b,c). We found this distance to be ~120-140 nm (Fig. 3d), which is very similar to what has been previously described for these proteins using STORM microscopy^{17,22}. Moreover, many of the presynaptic active zones (Bassoon stainings) appear to be segmented (Fig. 3b). The segments typically aligned with clusters of postsynaptic molecules (Homer 1 staining), as indicated by arrowheads in side views of synapses (Fig. 3b). This phenomenon, which may be important in regulating synaptic function by coordinating the positioning of pre- and postsynaptic elements, has been described only recently with advanced STORM microscopy²³. The lateral organization of these molecules may be even more complex, as revealed by face views of the synapses (see one example, as a z-stack, in Fig. 3c). These findings are again similar to previously described STORM results¹⁷. This type of information could not be obtained with either conventional microscopy or with classical 4x ExM (Supplementary Fig. 6). Overall, such examples demonstrate that X10 microscopy can reproduce results that were previously obtained only with highly specialized imaging tools. This also demonstrates that possible distortions at the nanometre level, where X10 should be most useful, seem to be so minimal that they do not become apparent in a comparison to other established super-resolution techniques. In addition, the ease with which multiple colours can be investigated in X10 is an advantage over previous localization microscopy methods, which have been typically limited to two colour channels in practice.

Other organelles, such as mitochondria, can be similarly investigated (Supplementary Figs. 7,8). Importantly, X10 microscopy can also be applied to thin tissue slices, where it provides the same resolution enhancement (Supplementary Fig. 9). For simplicity, we analysed the same markers as in Fig. 2, and we observed the same overall increase in image quality (Supplementary Fig. 9c).

X10 microscopy lags slightly behind in resolution compared to one other recently published advancement of ExM, namely iterative expansion microscopy (iExM)²⁰. In iExM, the classical 4x gel is applied to the same sample multiple times in sequence, to achieve a multiplication of the expansion factors of the individual gels. This approach yields an expansion factor of up to ~20x, with two iterations, which is sufficient to resolve the lumen of microtubules; something which is currently just beyond the reach of X10 (see Supplementary Fig. 5). However, iExM is much more variable in its expansion factor than X10, as the multiplication of two classical 4x ExM gels also results in a multiplication of the variability in their individual expansion factors, which usually spans from 3.5x to 4.5x^{1-4,20}. At the same time, the iterative protocol of iExM requires additional time and effort to break the first gel and make the second gel, and is not compatible with the use of conventional off-the-shelf antibodies, but requires custom-made DNA-oligo coupled antibodies²⁰. This makes iExM more laborious, more expensive, and more time consuming than X10. That said, it may be possible in the future to combine the X10 gel with the iExM principle to achieve lateral expansion factors of up to 100x.

X10 thus provides a toolset for a cheap (less than 2\$ for all reagents used in one experiment, except antibodies) and easy to use (no special machinery or custom antibodies required), multi-colour super resolution imaging, which can be performed on widely available epifluorescence setups. The resolution achieved rivals that of other nanoscopy techniques, which are currently not in universal distribution due to their specialized equipment requirements, high implementation and maintenance costs, and demand for specially trained personnel. At the same time, the resolution attained with X10 is on the order of the probe sizes (Supplementary Fig. 5), which renders it sufficient for super-resolution imaging within the limits imposed by the current imaging probe toolbox. Due to all of these arguments, X10 may facilitate a wider spread of super-resolution imaging than is currently possible. At the same time, the fact that this technique can only be applied to fixed samples remains a fundamental limitation, which cannot be overcome.

Combining X10 with physics-based super-resolution, and especially with a coordinate-targeted approach such as STED²⁴, which can be applied rapidly and efficiently to large imaging volumes, would provide an ultimate resolution equal to the size of the fluorophores. This should enable the investigation of molecular assemblies or molecule orientation more efficiently than virtually any other current tools, especially if probes smaller than antibodies are employed^{7,8,15}.

Acknowledgements: We thank Martin Helm for help with the STED imaging. S.T. was supported by an Excellence Stipend of the Göttingen Graduate School for Neurosciences, Biophysics, and Molecular Biosciences (GGNB). This work was supported by grants to S.O.R. from the European Research Council (ERC-2013-CoG NeuroMolAnatomy) and from the Deutsche Forschungsgemeinschaft (DFG): SFB 889/A5, 1967/7-1, and SFB1190/P09.

Author contributions: S.T. and D.C. performed the stainings. M.M. cultured COS7 cells, produced the labelled scFv for Tubulin stainings, and performed the STED imaging. H.W. performed the STORM imaging. S.T. performed all other experiments and the expansion microscopy imaging. S.T., S.K., and S.O.R. conceived the project. S.T and S.O.R. performed the data evaluation and wrote the manuscript.

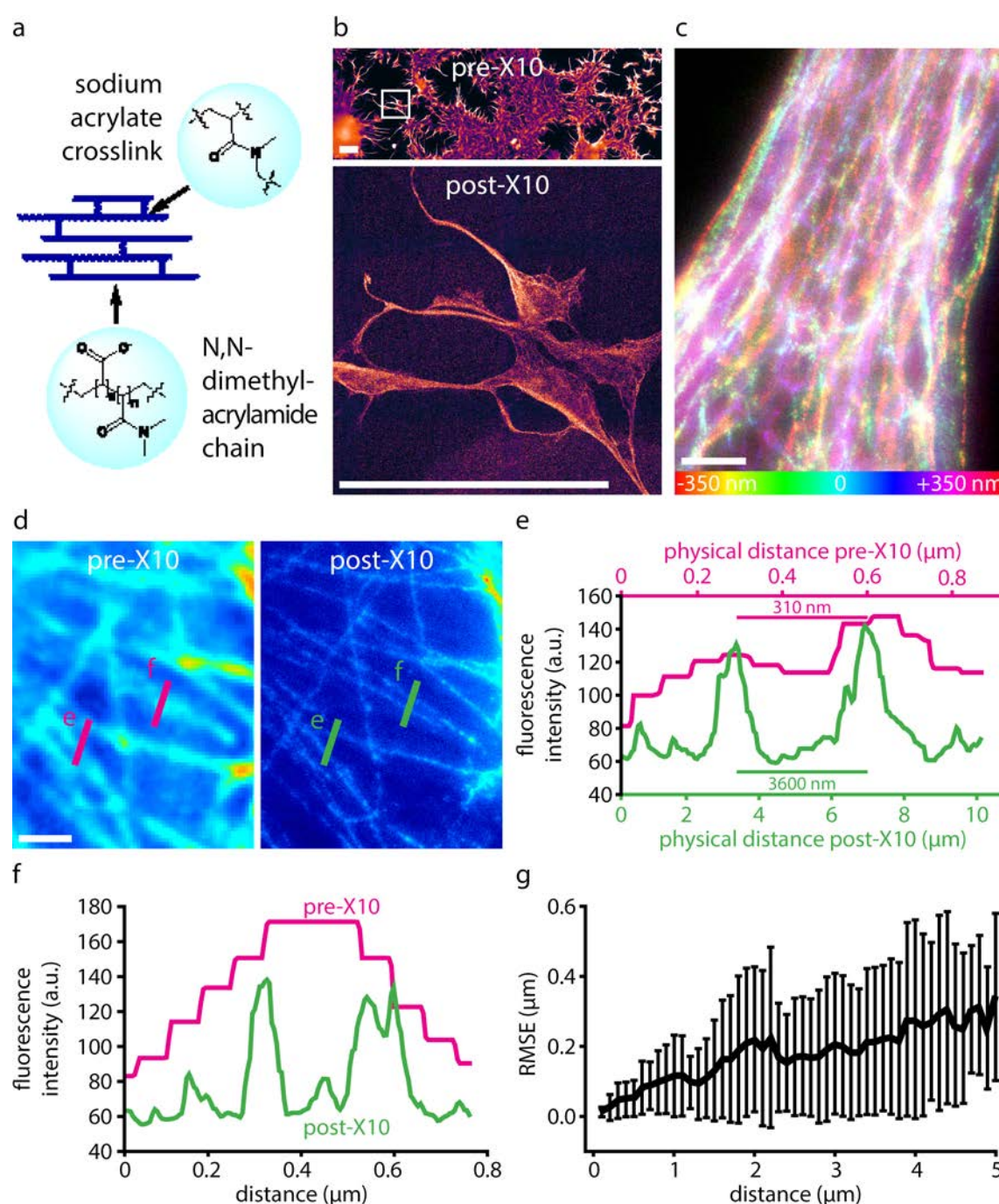


Figure 1: X10 achieves a resolution of 30 nm on conventional epifluorescence microscopes.

(a) The X10 gel is composed of *N,N*-dimethyl-acrylamide (DMAA) polymer chains and sodium acrylate (SA) crosslinks. Crosslinking of fluorophores to the gel is achieved by Acryloyl-X anchoring (Supplementary Fig. 1b), as previously described⁴.

(b) The X10 gel is swellable to >10x of its original size. The top panel shows an overview image of COS7 cells stained for Tubulin, before expansion. The bottom panel shows the cells framed in the top panel (white rectangle), after expansion. The images are to scale, demonstrating an expansion factor of 11.4x in this example. Note that both images are

stitched together from multiple imaging frames. Scale bars: 100 μm (both panels; the scale bars in post-X10 images shown in this paper always reflect the original physical dimensions, not the actual physical dimensions after expansion, unless noted otherwise).

(c) X10 microscopy reveals the 3D organization of the Tubulin network in COS7 cells. The relative axial position of the fluorophores is visualized in a z-stack projection by colour-coding (see scale at the bottom). Expansion factor: 11.4x. Scale bar: 1 μm .

(d) Comparison between pre-expansion resolution of Tubulin imaging in COS7 cells (left panel) and post-expansion resolution in the same sample (right panel). Note that the images have not been processed to minimize distortions or to achieve a better correlation. Expansion factor: 11.5x. Scale bar: 1 μm .

(e) An exemplary measurement for the X10 expansion factor. A line scan was drawn over corresponding regions before and after expansion, as indicated in panel (d) by the lower left lines. The scan encompasses two bundles of microtubules (magenta, before expansion; green, after expansion). Measuring the distances between the fluorescence peaks corresponding to the two microtubule bundles, before and after expansion, provides a simple estimate for the physical expansion achieved ($\sim 11.5\text{x}$, in this example).

(f) Another line scan analysis (upper right lines in panel (d)) demonstrates the typical gain of information achieved through X10: single peaks observed before expansion typically hide multiple elements that become evident after expansion.

(g) A root mean square error (RMSE) analysis of the distortions between aligned pre- and post-expansion images, such as those presented in (d), in X10 microscopy ($n = 3$ independent experiments).

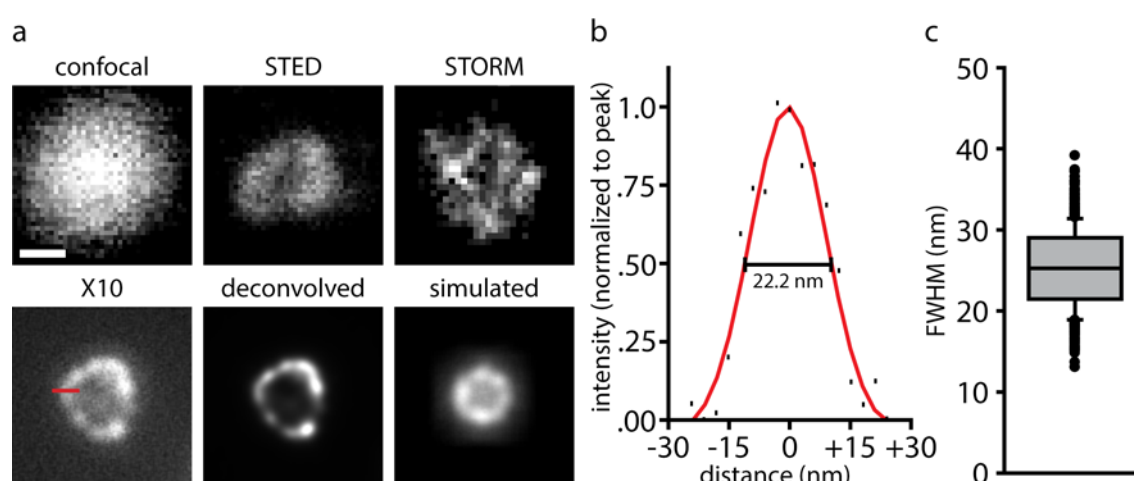


Figure 2: The resolution of X10 is ~25 nm.

(a) The resolution of X10 microscopy is at least ~25 nm. Shown here are stainings for Pmp70 in neurons. Pmp70 is a protein located on the membrane of peroxisomes, which have a size of 100-200 nm, making their sharply defined membrane edges convenient for resolution measurements. The panels show peroxisomes, from left to right and top to bottom: imaged with a confocal microscope before expansion, a STED microscope before expansion, a STORM microscope before expansion, an epifluorescence microscope after expansion, the same image after deconvolution, and a simulated peroxisome. Expansion factor: 9.5x. Scale bar: 100 nm (applies to all panels). The red line indicates a line scan over the peroxisome membrane (60 nm in length).

(b) The exemplary line scan from the X10 image in (a) with a best Gaussian fit curve, and the measurement of resolution as full width at half maximum (FWHM).

(c) A quantification of the average resolution, which is 25.2 ± 0.2 nm ($n = 653$ line scans from 2 independent experiments).

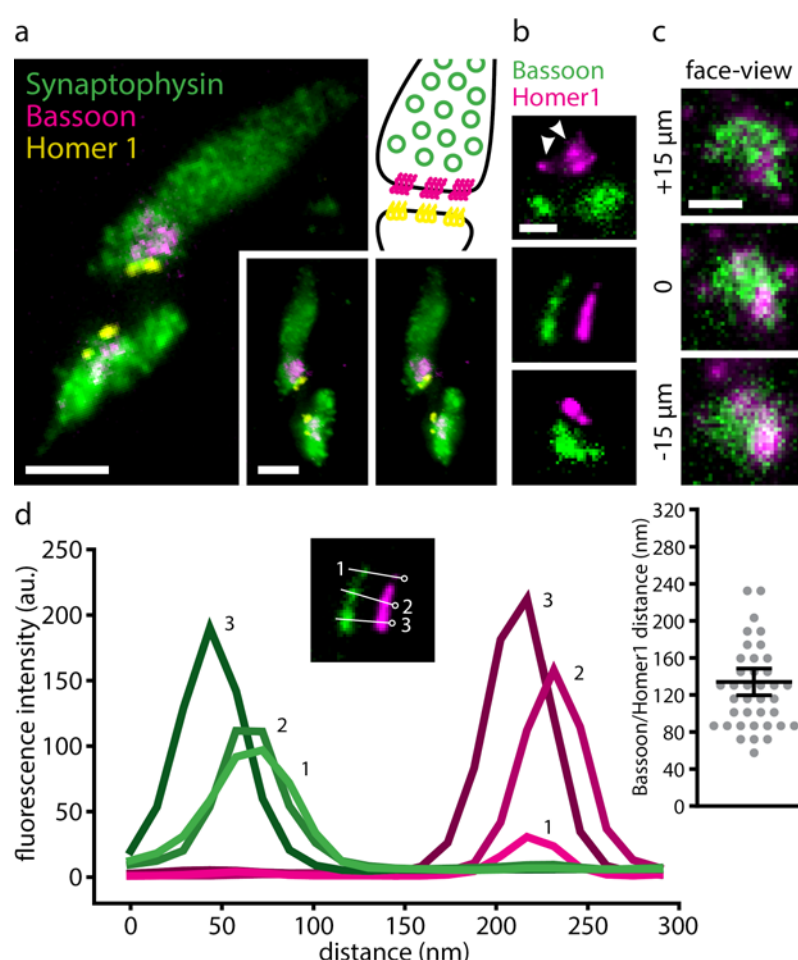


Figure 3: Multi-colour imaging with X10 reveals ultrastructural details in synapses.

(a) 3-colour imaging resolves synaptic vesicles (identified by Synaptophysin), along with presynaptic active zones (identified by Bassoon) and postsynaptic densities (identified by Homer 1). The panel at the top right gives a schematic overview of the organization of a synapse, for orientation (colours as in the fluorescence images). The 2 panels on the bottom right provide a stereo view of the synapses. Expansion factor: 11.0x. Scale bars: 500 nm (both).

(b) Higher-magnification images show the alignment of presynaptic active zones and postsynaptic densities, as well as the distance between them, in side-view. Expansion factor: 11.0x. Scale bar: 200 nm.

(c) A z-stack through an additional synapse, in face-view. Expansion factor: 11.0x. Scale bar: 200 nm.

(d) Line scans through presynaptic active zones and through the corresponding postsynaptic densities reveal the distance between the two. The image inset shows three example line scans, and identifies them by number (green is Bassoon, magenta is Homer 1). The inset on the right quantifies the range of observed distances ($n = 38$ active zones and corresponding postsynaptic densities; mean \pm SEM are 127 ± 7.1 , indicated by the black lines).

References

1. Chen, F., Tillberg, P. & Boyden, E. Expansion microscopy. *Science* (80-.). **347**, 543–548 (2015).
2. Chozinski, T. J. *et al.* Expansion microscopy with conventional antibodies and fluorescent proteins. *Nat. Methods* **13**, 485–488 (2016).
3. Chen, F. *et al.* Nanoscale imaging of RNA with expansion microscopy. *Nat. Methods* 1–9 (2016). doi:10.1038/nmeth.3899
4. Tillberg, P. W. *et al.* Protein-retention expansion microscopy of cells and tissues labeled using standard fluorescent proteins and antibodies. *Nat. Biotechnol.* **34**, 987–992 (2016).
5. Cipriano, B. H. *et al.* Superabsorbent hydrogels that are robust and highly stretchable. *Macromolecules* **47**, 4445–4452 (2014).
6. Tillberg, P. W. *et al.* Protein-retention expansion microscopy of cells and tissues labeled using standard fluorescent proteins and antibodies. *Nat. Biotechnol.* **13**, 1–9 (2016).
7. Ries, J., Kaplan, C., Platonova, E., Eghlidi, H. & Ewers, H. A simple , versatile method for GFP-based microscopy via nanobodies. *Nat. Methods* **9**, 582–584 (2012).
8. Fornasiero, E. F. & Opazo, F. Super-resolution imaging for cell biologists. *Bioessays* 436–451 (2015). doi:10.1002/bies.201400170
9. Wildanger, D., Rittweger, E., Kastrup, L. & Hell, S. W. STED microscopy with a supercontinuum laser source. *Opt. Express* **16**, 358–362 (2008).
10. Wildanger, D., Bückers, J., Westphal, V., Hell, S. W. & Kastrup, L. A STED microscope aligned by design. *Opt. Express* **17**, 209–213 (2009).
11. Wegel, E. *et al.* Imaging cellular structures in super- resolution with SIM, STED and Localisation Microscopy: A practical comparison. *Sci. Rep.* 1–13 (2016). doi:10.1038/srep27290
12. Niehörster, T. *et al.* Multi-target spectrally resolved fluorescence lifetime imaging microscopy. *Nat. Methods* **13**, 257–262 (2016).
13. Bálint, S., Vilanova, I. V., Álvarez, S. Á. & Lakadamyali, M. Correlative live-cell and superresolution microscopy reveals cargo transport dynamics at microtubule intersections. *Proc. Natl. Acad. Sci. U. S. A.* **110**, 3375–3380 (2013).

14. Bates, M., Huang, B., Dempsey, G. T. & Zhuang, X. Multicolor Super-Resolution Imaging with Photo-Switchable Fluorescent Probes. *Science (80-.)*. **317**, 1749–1752 (2007).
15. Mikhaylova, M. *et al.* Resolving bundled microtubules using anti-tubulin nanobodies. *Nat. Commun.* **6**, 1–7 (2015).
16. Huang, B., Jones, S. A., Brandenburg, B. & Zhuang, X. Whole-cell 3D STORM reveals interactions between cellular structures with nanometer-scale resolution. *Nat. Methods* **5**, 1047–1052 (2008).
17. Dani, A., Huang, B., Bergan, J. & Dulac, C. Super-resolution Imaging of Chemical Synapses in the Brain. *Neuron* **68**, 843–856 (2010).
18. Schmidt, R. *et al.* Spherical nanosized focal spot unravels the interior of cells. *Nat. Methods* **5**, 539–544 (2008).
19. Balzarotti, F. *et al.* Nanometer resolution imaging and tracking of fluorescent molecules with minimal photon fluxes. *Science (80-.)*. **9913**, (2016).
20. Chang, J. *et al.* Iterative expansion microscopy. *Nat. Methods* **14**, 593–599 (2017).
21. Gao, R., Asano, S. M. & Boyden, E. S. Q&A: Expansion microscopy. *BMC Biol.* **15**, 1–9 (2017).
22. Glebov, O. O., Cox, S., Humphreys, L. & Burrone, J. Neuronal activity controls transsynaptic geometry. *Sci. Rep.* 1–11 (2016). doi:10.1038/srep22703
23. Tang, A. *et al.* A trans-synaptic nanocolumn aligns neurotransmitter release to receptors. *Nature* **536**, 210–214 (2016).
24. Hell, S. W. Far-Field Optical Nanoscopy. *Science (80-.)*. **316**, 1153–1158 (2007).